

## Supporting Information for “Differences in mechanical properties lead to anomalous phase separation in a model cell co-culture”

Supravat Dey\* and Moumita Das†

*School of Physics and Astronomy, Rochester Institute  
of Technology, Rochester, New York 14623, USA.*

(Dated: December 18, 2020)

### Abstract

List of Supplementary Files.

1. Movie showing phase separation for the parameters given in the main manuscript.
2. Additional results on the origin and robustness of the results for unusual the phase separation behavior discussed in the main manuscript.

## ADDITIONAL RESULTS ON THE ORIGIN AND ROBUSTNESS OF THE UNUSUAL PHASE SEPARATION REPORTED IN THE MAIN MANUSCRIPT

We present results for the following cases.

1. Both  $h$  and  $c$  cells have the same Young's modulus and surface energy.
2. Both  $h$  and  $c$  cells have the same Young's modulus but different surface energy.
3. Changes in rotational diffusivity
4. A passive system.

### 1. The $h$ and $c$ cells have the same stiffness and surface energies, and prefer homotypic contact to heterotypic contact.

Here, we have assumed that the  $h$  and  $c$  cells have the same Young's modulus,  $Y_h = Y_c = 1.5 \text{ nN}\mu\text{m}^{-2}$ , and the surface energy for homotypic contacts are the same,  $\sigma_{hh} = \sigma_{cc} = 0.5 \text{ nN}\mu\text{m}^{-1}$ . The surface energy for heterotypic contact  $\sigma_{hc} = 0.1\sigma_{hh}$ , i.e.  $\sigma_{hc} < \sigma_{hh}$ . The other parameter values are the same as in the Table in the main manuscript. Our results are shown in Fig. S1.

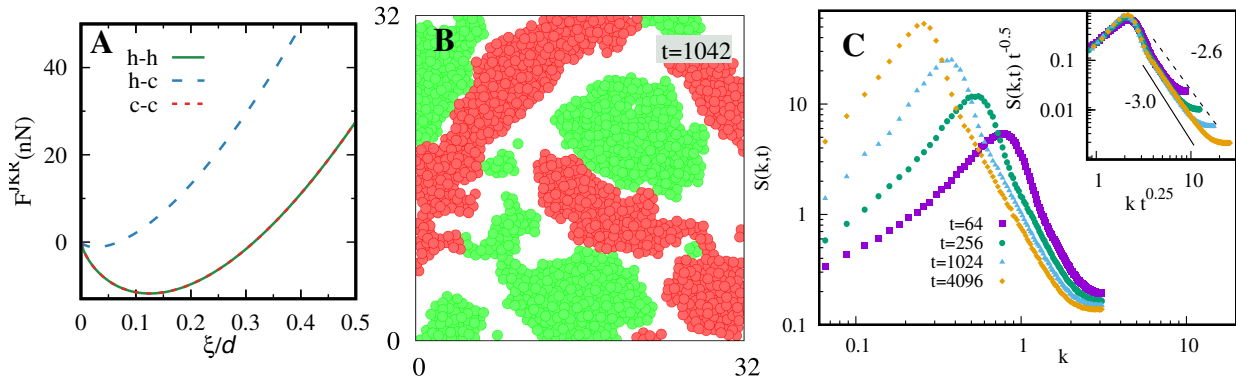


FIG. S1. **Cell types with identical homotypic contacts show usual phase-separation.** (A) The JKR force for different contacts. (B) A typical snapshot at  $t = 1024$ . (D) The structure factors for both the  $h$  and  $c$  cell clusters are identical. Inset:  $S(k, t)$  at different times are scaled with  $t^{0.25}$ , as one would expect from usual conserved dynamics. The power-law with decay exponents of 3 and 2.6 are drawn. The large- $k$  scaled structure factor seems to follow the exponent 3.

The curves for the JKR force between two cells as a function of their overlap distance are identical for  $h-h$  and  $c-c$  contacts, and at small overlap distances, this force is much more strongly attractive than for  $h-c$  contact. In this case, both the  $h$  and the  $c$  cells form compact, cohesive clusters, and the density structure factor obeys Porod law, as is typically observed in phase separation in binary systems. The cluster sizes for both cell types follow the growth law  $t^{0.25}$ .

**2. The  $h$  and  $c$  cells have the same stiffness, but different surface energies. They prefer homotypic contact to heterotypic contact.**

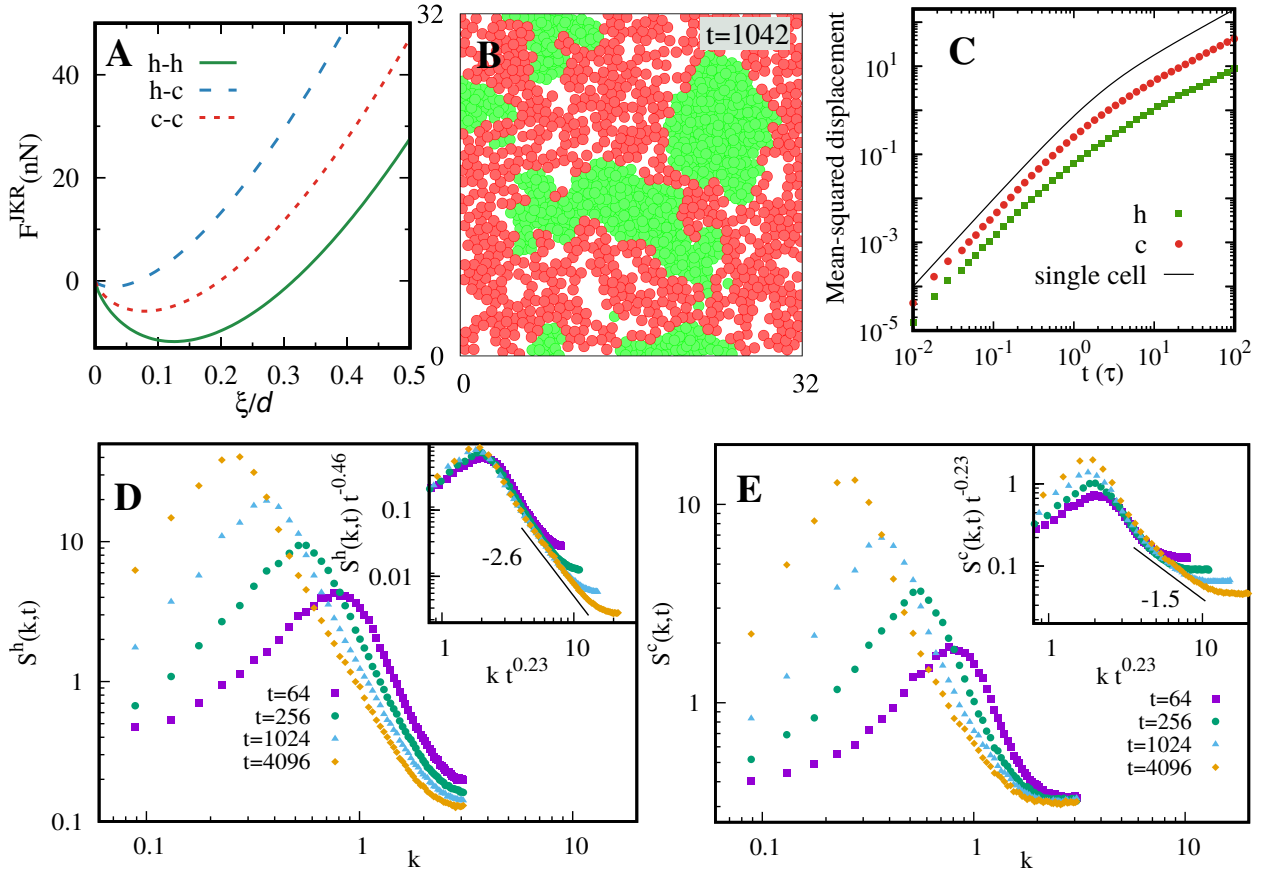


FIG. S2. **Difference in surface energies can lead to unusual phase-separation.** (A) The JKR force. (B) A typical snapshot at  $t = 1024$ . (C) The mean square displacement show faster motion for  $c-$  cell types. The structure factors for  $h$  cells (D), and  $c$  cells. Insets:  $S(k, t)$  at different times are scaled with  $t^{0.23}$ . The large- $k$  scaled structure factors show different behavior for  $c$  and  $h$  cells, representing disperse and compact clusters.

We assume  $Y_h = Y_c$  and  $\sigma_{hh} < \sigma_{cc} < \sigma_{hc}$ . For the results shown in Fig. S2, we choose  $Y_c = 1.5 \text{ nN}\mu\text{m}^{-2}$ , with the rest of the parameters being the same as in the Table in the main manuscript. The differences in surface energies leads to different JKR forces for  $h-h$ ,  $c-c$ , and  $h-c$  contacts. We find that the  $h-h$  contact force curve lies below the  $c-c$  force curve for all overlap distances – i.e. the  $h-h$  force is more attractive than the  $c-c$  force at small overlap distances as in the main manuscript, but unlike that case it is less repulsive at larger distances. The phase separated clusters form compact and dispersed morphologies for  $h$  and  $c$  cells as in the paper. The decay exponent for the structure factor of  $c$  cells is found to be 1.5, i.e. the departure from the Porod law value of 3 is little different than in the main manuscript (1.1). The mean squared displacement show similar behavior. Recall that in the main manuscript, the cell stiffness is different for  $h$  and  $c$  cell types.

### 3. Changes in rotational diffusivity

In our model, the only source of noise is rotational diffusion. This diffusivity should be sufficiently large to observe clear phase-separation in a homogenous binary mixture. Here, we present the results for values of  $D_r$  smaller and larger than that used in Table-1 of the main manuscript: (i)  $D_r = 0.025 \text{ min}^{-1}$  (0.5 times the value in Table-1) and (ii)  $D_r = 0.1 \text{ min}^{-1}$  (twice the value in Table-1). The top panel of Fig. S3 shows the configuration snapshot and structures factors for  $D_r = 0.1 \text{ min}^{-1}$ , while the bottom panel shows the corresponding plots for  $D_r = 0.025 \text{ min}^{-1}$ . For the larger value of  $D_r$ , we observe the same growth law and structure factors with the same decay exponents as in the main paper. However, for the smaller  $D_r$  value, the cluster morphologies for both cell types are very disordered and amorphous. The data collapse is also poor, and the decay exponents for structure factor are different.

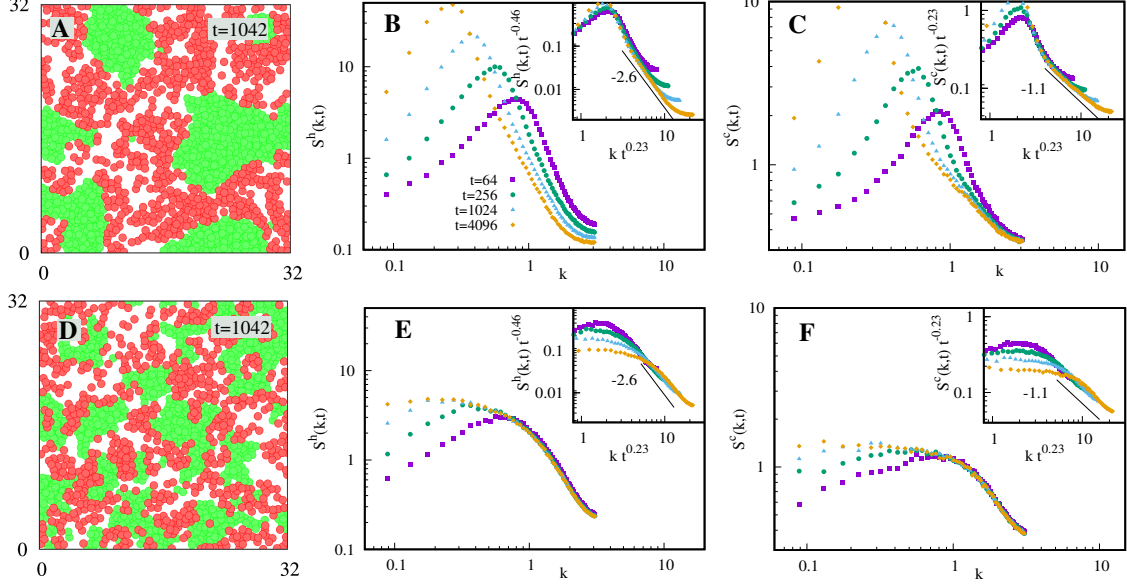


FIG. S3. **Results for two different rotational diffusivities,  $D_r = 0.1 \text{ min}^{-1}$  (Top panel) and  $D_r = 0.025 \text{ min}^{-1}$  (bottom panel).** Figures (A) and (D) show the configuration snapshots at  $t = 1024$ , (B) and (E) show unscaled and scaled structure factors for  $h$ -cells, and (C) and (F) show the scaled and unscaled structure factors for  $c$ -cells. Larger, more well-defined clusters are observed for (A) than (D), and data collapse in (B) and (C) are far better than in (E) and (F). Data was obtained for  $L = 128$ . Other parameters same as in Table-1.

#### 4. Passive case

To understand the role of activity, we study a passive system. Here, the self-propelled velocity  $v_0 = 0$ . The equation of motion of a cell  $i \in \{1, N\}$

$$\frac{d\vec{r}_i}{dt} = \mu \sum_{j \in n_i} \vec{F}_{ij}^{\text{JKR}} + \sqrt{2D_T} \vec{\eta}_{T,i}(t). \quad (\text{S1})$$

The random vector  $\vec{\eta}_{T,i}(t)$  is translational noise. It has zero mean and is  $\delta$ -correlated i.e.,  $\langle \eta_{T,i}^\alpha(t) \rangle = 0$  and  $\langle \eta_{T,i}^\alpha(t) \eta_{T,j}^\beta(t') \rangle = \delta_{i,j} \delta_{\alpha\beta} \delta(t - t')$  and  $D_T$  is the translational diffusivity.

In Fig. S4, we plot the results for the passive case. Our results still show distinct morphologies for  $h$ - and  $c$ -cell clusters, but the cluster formation for  $c$  cells are less well-defined than the active case.

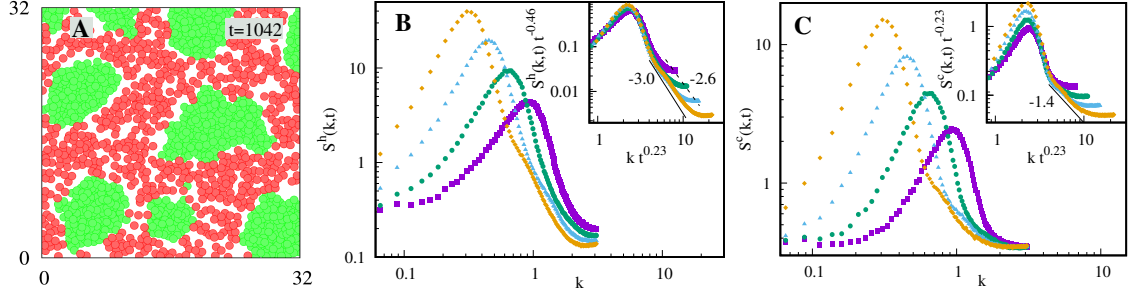


FIG. S4. Results for the passive case. (A) Snapshot at  $t = 1024$ . (B) Unscaled and scaled (inset) structure factor for  $h$  cells. (C) Unscaled and scaled (inset) structure factor for  $c$  cells. Parameters:  $D_T = 2.0 \mu\text{m}^2 \text{min}^{-1}$ , and rests are taken from Table-1.